

CHARACTERISTICS OF THE INITIAL DENSIFICATION PROCESSES OF SNOW / FIRN IN WILKES LAND, ANTARCTICA

Qin Dahe¹ and N.W. Young²

¹Lanzhou Institute of Glaciology and Geocryology, Academia sinica, Lanzhou, China 730000

²Antarctic Divison, Kingston, Tasmania 7150, Australia

Abstract 14 shallow snow / firn cores were taken by drilling with the PICO lightweight hand coring auger on Law Dome and Wilkes Land along a line approximately 111°E longitude between 66°S and 74°S latitude. 5 of these cores, BJ, LJ24, GC30, GC40 and GC46, 20–30 m deep, are studied in detail in this paper. The densities of snow / firn were measured in a cold room at temperature between -18°C and -14°C by taking consecutive core samples and weighing the mass of each sample whose volume was known. The characteristics of the initial densification (till a density of 550 kg / m^3) including the variation of snow / firn density with increasing depth, densification rate of snow / firn and the compactive viscosity coefficient of snow / firn are studied, and the factors affecting this initial densification process are discussed. From the obtained measurements, a relationship between compactive viscosity coefficient of snow / firn and mean annual temperature is found in case $\rho=550 \text{ kg / m}^3$. For snow / firn on Wilkes Land, the relationship we found at a mean annual temperature below -25°C (i.e. no melting features are present in stratigraphy) is very similar to that found by Nishimura and others (1983) on Mizuho Plateau, Antarctica.

Key words Wilkes Land snowfirn densification

Introduction

The densification process starts as soon as new snow is deposited on the surface of ice sheet. It is a complex process involving changes in crystal size, shape, orientation and other microproperties, resulting in variation of density with depth. Previous studies have described the densification process variously as diagenesis (Anderson and Benson, 1963), metamorphism (Liboutry and Duval, 1985), sintering (Maeno, 1982), etc.

It has been suggested that the densification from snow to ice be divided into three stages. In the initial stage the new snow crystals deposited on the surface undergo mechanical destruction and packing until the density reaches about 550 kg / m^3 . In this article the discussion is only concerned in this initial stage of the densification.

Description of Coring Sites

During 1984 ANARE, 14 shallow snow / firn cores were taken by drilling at 12 sites on Law Dome, along an oversnow traverse south of Casey on Wilkes Land. 5 of them were taken at three sites, i.e. Lanyon Junction (LJ), LJ24 and Blyth Junction (BJ), On the western side of Law Dome. The other 9 were taken along the IAGP traverse route between 110°E and 112°E longitude as far as $74^{\circ}08'\text{S}$ latitude. The core length ranges from 11m at GC36 to about 30m at LJ24. Among them 5 cores with a length of 20m or more, named LJ24, BJ, GC30, GC40 and GC46, are discussed in detail. The ages of these 5 cores are estimated to

be 40 years for GC30 and about 140 years for LJ24. The 12 coring sites were set in a wide area with different geographic conditions (Table 1).

Table 1. Basic physical geographic conditions of the coring sites.

Station	Latitude and longitude	Dist from coast (km)	Elev. (m)	Mean annual temp. (°C)	Mean annual accum. (kg / m ² ·a)
LJ	66°19'S, 110°52'E	15	473	-12.6	100
LJ24	66°23'S,111°22'E	38	765	-15.5	/
BJ	66°28'S,111°58'E	63	1043	-17.7	77
GC30	69°21'S,111°51'E	425	2117	-33.6	248
GC36	69°48'S,112°01'E	481	2307	-36.3	190
GC37	70°09'S,111°50'E	514	2430	-38.0	170
GC38	70°27'S,111°44'E	544	2523	-39.4	190
GC40	71°10'S,111°22'E	624	2694	-43.6	130
GC42	72°03'S,110°55'E	725	2810	-46.7	80
GC44	72°26'S,110°42'E	769	2837	-48.3	100
GC47	73°42'S,110°12'E	913	3044	-52.1	70
GC46	74°08'S,109°50'E	964	3090	-52.5	70

Density-Depth Profile

The density measurement of snow / firn was made in a cold room at a temperature between -18°C and -14°C, by taking consecutive samples from the core and weighing the mass of each sample whose volume was known (Qin, in press). Total 7162 samples were measured. The detailed density-depth profiles of three typical cores are shown in Fig. 1. The density tends to increase with increasing depth, but the increasing rate varies markedly from site to site.

For LJ the density values are scattered on the right side in Fig. 1a. Many infiltration ice layers and lenses can be found in the firn, which provides an evidence for surface melting during the warmer months. For GC30 the density values are regularly scattered in a certain area, as shown in Fig. 1b which is a typical density-depth profile for the inland shallow snow / firn cores. The scatter of density values in Fig. 1c is mostly similar to that in Fig. 1b except a few density values on the right side of the figure because of the melting features.

There is a pattern of the variation in the mean density, for example, the mean density in the uppermost one metre at LJ, LJ24, BJ, GC40, GC42, GC44, GC47 and GC46 are 560, 470, 420, 400, 370, 380, 390 and 400 kg / m³, respectively (Fig. 2), which shows that the mean density in the top one metre decreases essentially from the north to the south. The mean density $\bar{\rho}_1$ in the uppermost one metre and the mean annual temperature, T , can be expressed by the following formular:

$$\bar{\rho}_1 = 346.28 \exp(-5.1 / T) \quad (1)$$

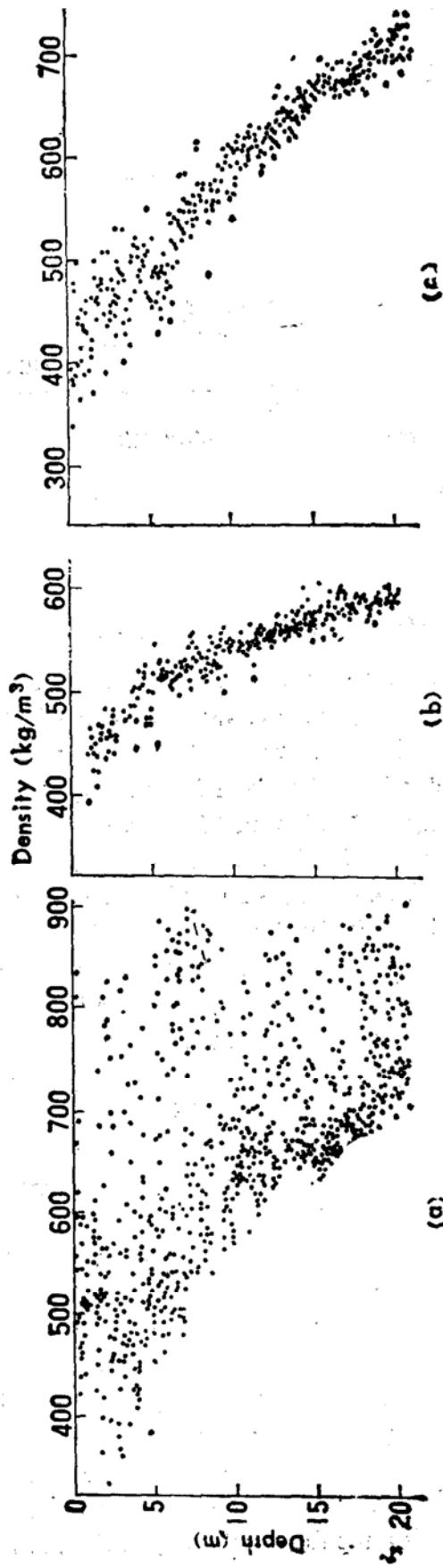


Fig. 1. The profiles of density versus depth for snow / firn cores LJ (a), GC30 (b) and BJ (c).

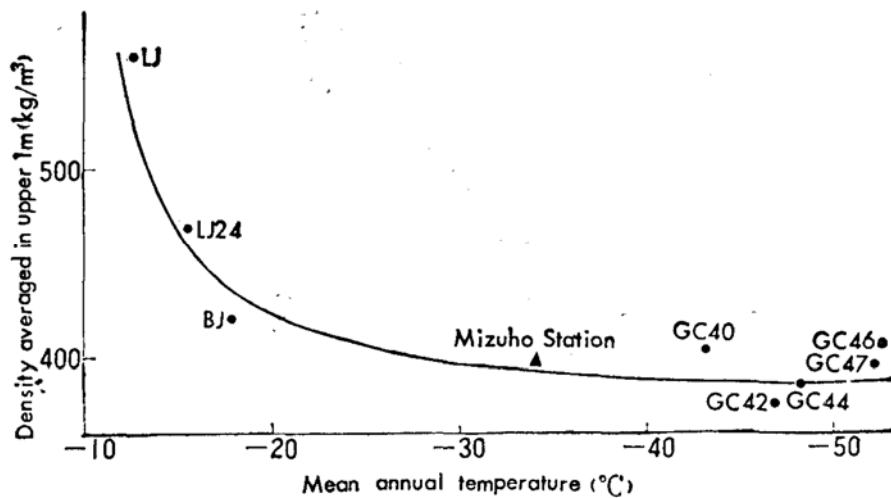


Fig. 2. Mean density averaged over the uppermost 1 m versus the mean annual temperature.

Magnitude of the Variation in Density

There is also a fluctuation in the density at every depth interval as shown in Fig. 1.

Gow (1968) has determined the magnitude of variation in density for the core from Byrd Station (80°S , 120°W , mean annual temperature -28.2°C , accumulation rate $140 \text{ kg / m}^2 \cdot \text{a}$). He found the variation in density differs from layer to layer, for example, it is about 100 kg / m^3 near the surface, 30 kg / m^3 at 3–4 m, 15 kg / m^3 at 10 m, and rarely exceeds 10 kg / m^3 at 20 m depth. The amplitude of variation tends to reduce rapidly with increasing depth. At Mizuho Station ($70^{\circ}42'\text{S}$, $44^{\circ}20'\text{E}$, -33.0°C , $70 \text{ kg / m}^2 \cdot \text{a}$) Maeno and Narita (1979) have found that the variation in density is in a range from 200 kg / m^3 near the surface, 100 kg / m^3 at 5 m, 40 kg / m^3 at 20 m to 20 kg / m^3 at 30 m depth.

Fig. 3 shows the density range between the maximum and the minimum values in one metre interval for the three longest cores from the inland, i.e. GC30, GC38 and GC46, together with the values from Byrd and Mizuho. The density range near the surface increases from less than 100 kg / m^3 at GC30, to more than 150 kg / m^3 at GC46. This difference in the density range, to a small extent, can be found at the bottom of the cores. Fig. 3 also shows that the density range at the sites reported in this work apparently reduces with the depth, but less rapidly than that at Byrd or Mizuho stations. This difference may possibly be explained from different thickness for measurement. In this work at least seven samples can be cut out for an annual layer. For the Byrd sample, thickness for density measurement is 10–250 mm, i.e. 1000 samples have been cut out from a core of 100 m. For Mizuho, 1533 samples have been cut out from a core of 60 m. Thus few samples have been covered in an annual layer, producing the substantial variation in density concealed.

Fig. 3 also shows that the density ranges at every depth interval increase from GC30 to GC46, associating with a reduction in the accumulation rate and the mean annual temperature. For the shallow snow / firn core, the overburden load on the densification can be neglected. Therefore the temperature is a top factor affecting on the densification of snow.

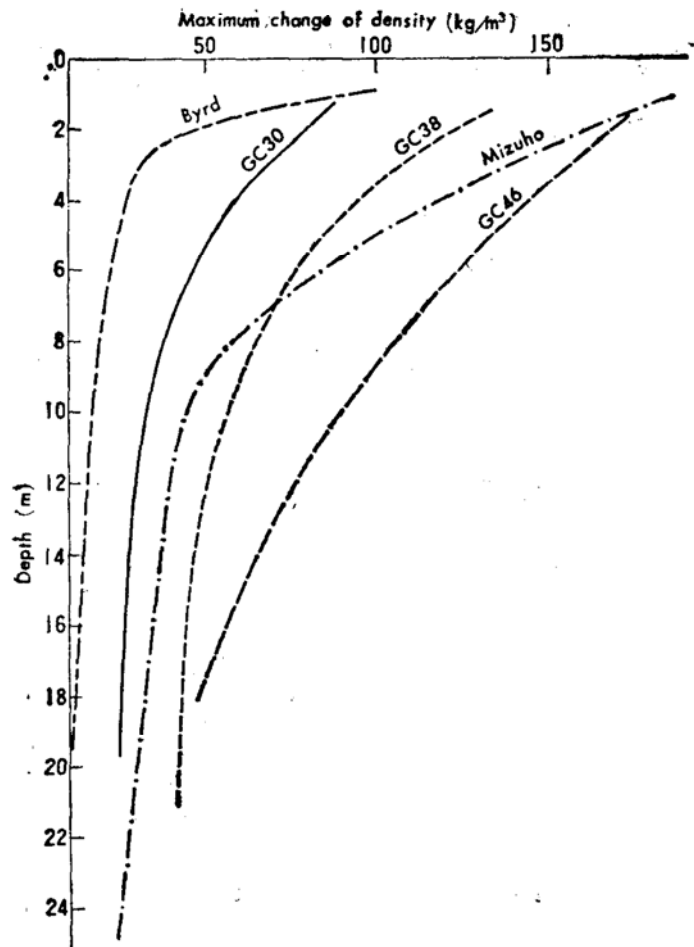


Fig. 3. Relationship between the magnitude of the metric variation in density and depth.

The Densification Rate

The curvatures and the slopes of the density-depth curves in Fig. 1a-b are different from site to site. In general, the curvature of the curves, i.e. the densification rate, decreases from north to south, which shows that the densification process is dependent on the temperature.

The densification rate, $\dot{\rho}$, can be defined as follows:

$$\dot{\rho} = d\rho / dt \quad (2)$$

where t is time (a) and ρ is density (kg / m^3).

Fig. 4 shows the mean densification rate over the first 40 years as a function of temperature for each of the sites. $\dot{\rho}$ is obviously dependent on the temperature for the inland sites. While results obtained at those sites close to the coast, for example LJ, do not coincide with the curve. It shows a strong relationship between $\dot{\rho}$ and the temperature in the shallow layer of the ice sheet. But the concept of densification is not suitable to the stratigraphy with melting features.

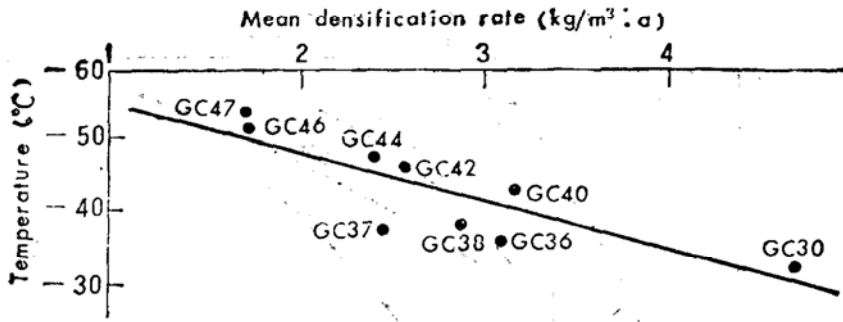


Fig. 4. Mean densification rate of snow / firn versus the mean annual temperature.

Compactive Viscosity Coefficient of Snow / Firn

The strain rate, $\dot{\epsilon}$, of snow after Yosida and others (1956) and Bader (1960) can be expressed as follows:

$$\dot{\epsilon} = -\frac{\sigma}{\eta} = -\frac{1}{\rho} \frac{d\rho}{dt} \quad (3)$$

where σ is the pressure of the overburden load on snow, and η is the compactive viscosity. It has been found that a linear relation exists between σ and η when the overburden load is approximately below 10 kg/m^2 (Nishimura *et al.* 1983), and that we measured is below this magnitude.

The time scale (t) can be calculated as follows:

$$t = \frac{1}{A} \int_0^z \rho(z) dz \quad (4)$$

where A is the mean accumulation rate, accounted as a constant for a given period, z the depth. Drawing a straight line to fit to the density versus age, the $\dot{\epsilon}$ value can be calculated for each depth by equation (3). The overburden load on snow can be calculated as:

$$\sigma = \int_0^z \rho(z) dz = \bar{\rho} z \quad (5)$$

where $\bar{\rho}$ is the mean density from snow surface to depth z , and easy to get from the consecutive density measurements.

Thus the compressive viscosity coefficient η can be estimated from η and $\dot{\epsilon}$ for each density. There is, however, a certain error in this method for determining η , because of uncertainty in determining the linear relation between density and age.

Moreover, Kojima (1964) and Nishimura and others (1983) described the coefficient as follows:

$$\eta = \eta_0 \exp\left(\frac{E}{KT}\right) \exp(b\rho) \quad (6)$$

where T and K are absolute temperature and the Boltzman constant respectively, b and E constants also. From Eq. (6).

$$b = \frac{\ln(\eta) - \ln(c)}{\rho} \quad (7)$$

where C is a constant when T is a constant. That is, b is the slope of the linear relationship between the logarithm of viscosity and density. Fig. 5 shows this relation between η and ρ for GC30, GC38, GC40 and GC46. The value of $\ln(\eta)$ increases with the increasing depth, approximately linear for all stations, but b varies from station to station, is $3.76 \times 10^{-2} \text{ m}^3/\text{kg}$ at GC30, 2.62×10^{-2} at GC38, 3.02×10^{-2} at GC40 and 3.28×10^{-2} at GC46, with a mean value of $3.17 \times 10^{-2} \text{ m}^3/\text{kg}$.

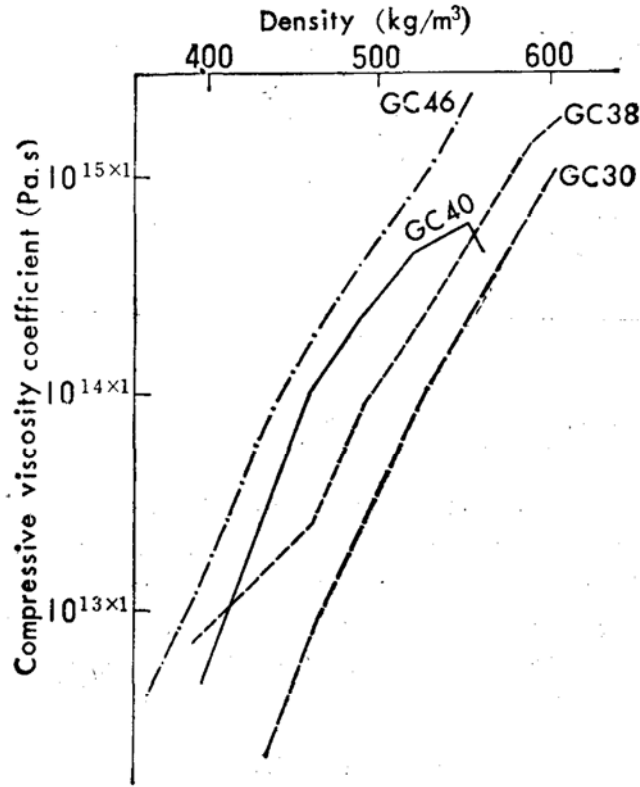


Fig. 5. The relationship between compressive viscosity coefficient (logarithm) and density of snow / firn on Wilkes Land, Antarctica.

In addition, from equation (6), we get:

$$\ln(\eta) = C_1 / T + C_2 \quad (8)$$

where $C_1 = E/k$, $C_2 = \ln(\eta_0) + b\rho$. The equation indicates that the relationship between $\ln(\eta)$ and $1/T$ is also linear when ρ is a constant. In case $\rho = 500 \text{ kg/m}^3$ the relationship between compressive viscosity coefficient and temperature for cores from Mizuho Plateau and the land of present study are shown in Fig. 6.

In Fig. 6 two different regression lines, are shown, one is derived from four stations on Mizuho Plateau, another from four stations on Wilkes Land. For discussing these two lines (dashed lines in Fig. 6), the physico-geographical conditions of these four stations on Mizuho Plateau are given in Table 2. As shown in Table 2, the mean annual temperatures at these four stations are below -33°C , except S18 where the temperature is -15.9°C . The stratigraphy of snow / firn on the northern Wilkes Land has been studied, where the mean an-

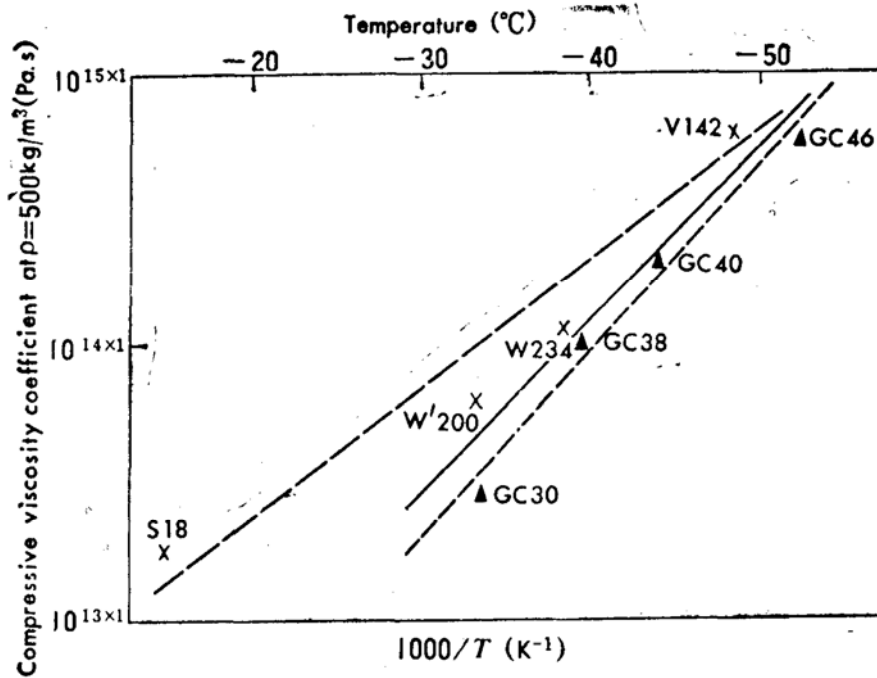


Fig. 6. Compactive viscosity coefficient at $\rho=500 \text{ kg / m}^3$ versus reciprocal of the kelvin temperature.

nual temperature is about -15°C and strong melting feature is found (Qin, in press). It shows that the snow / firn in vertical direction is inhomogeneous and this property should have effect on the compressive viscosity of snow / firn. Conversely, the highest temperature is always below the melting point when the mean annual temperature is below -25°C at the places of Antarctica. According to the meteorologic data such as the mean annual temperature was -33.0°C from 1977 to 1983, the maximum temperature was -4.8°C (January 20,

Table 2. Basic physicogeographic conditions for the stations on Mizuho Plateau*.

Station	Elev. (m)	Latitude and longitude	Mean annual temp. ($^\circ\text{C}$)	Mean annual accumulation rate ($\text{kg / m}^2 \cdot \text{a}$)
S18	600	$69^\circ 02' \text{S}, 40^\circ 07' \text{E}$	-15.9	210
W'2000	2000	$69^\circ 35' \text{S}, 48^\circ 50' \text{E}$	-33.1	290
U234	2640	$71^\circ 01' \text{S}, 47^\circ 29' \text{E}$	-38.5	190
V142	3076	$72^\circ 32' \text{S}, 51^\circ 57' \text{E}$	-48.1	90

* After Nishimura *et al.*, 1983.

1979) and still below the melting point during the seven years at Mizuho Station¹⁾. For this reason, there were no melting features in the stratigraphies of the seven stations in Fig. 6. Taking no account of S18, the relationship between logarithmic compressive viscosity coefficient and the reciprocal of the Kelvin temperature can be expressed by one regression line (the middle line in Fig. 6). It illustrates that the obtained compressive viscosity of snow / firn

1) See JARE Data Report, No. 47, 52, 57, 65, 86 and No. 101.

is suitable for those places in Antarctica, where the mean annual temperature is below -25°C as same as the study of the relationship between η and T in snow in East Antarctica.

Acknowledgements The authors express their sincere thanks to Dr. Ian Allison. Prof. Huang Maohuan, Mr. Wang Wenti and Mr. Han Jiankang for their helpful discussions and comments, and Ms. Jin Zhenmei for drawing illustrations.

References

- Anderson, D.L., Benson, C.S. (1963): The densification and digenesis of snow, *In* Kingery, W.D. (ed), *Ice and Snow*, M.I.T. Press, 391-411.
- Bader, H. (1960): Theory of densification of dry snow on high polar glaciers, SIPRE RR 69.
- Gow, A.J. (1968): Deep core studies of the accumulation and densification of snow at Byrd Station and Little America V, Antarctica. CRREL RR 197.
- Kojima, K. (1964) Densification of snow in Antarctica, *In* Mellor, M. (ed), *Antarctic Snow and Ice Studies*, Antarctic Research Series 2, 157-218.
- Lliboutry, L., Duval, P. (1985): Various isotropic and anisotropic ices found in glaciers and polar ice capes and their corresponding rheologies, *Annales Geophysicae*, 3(2), 207-224.
- Meano, N., Narita, N. (1979): Compactive viscosity of snow and its climate implications at Mizuho Station, Antarctica, *Antarctic Record*, 67, 18-31.
- Meano, N. (1982): Densification rates of snow at polar glaciers, *Memoirs of National Institute of Polar Research, Special Issue*, 24, 204-211.
- Nishimura, H., Maeno, N., Satow, K. (1983): Initial stage of densification of snow in Mizuho Plateau, Antarctica, *Memoirs of National Institute of Polar Research, Special Issue*, 29, 149-158.
- Yosida, Z., Oura, H., Kuroiwa, D., Huzioka, T., Kojima, K., Aoki, S., Kinoshita, S. (1956): Physical studies on deposited snow, II. Contribution from the Institute of Low Temperature Science, Hokkaido University, No. 9.

(Received December, 1990)